

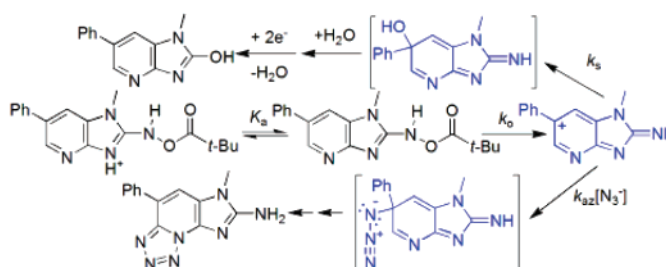
Synthesis and Decomposition of an Ester Derivative of the Procarcinogen and Promutagen, PhIP, 2-Amino-1-methyl-6-phenyl-1*H*-imidazo[4,5-*b*]pyridine: Unusual Nitrenium Ion Chemistry

Thach-Mien Nguyen and Michael Novak\*

Department of Chemistry and Biochemistry, Miami University, Oxford, Ohio 45056

novakm@muohio.edu

Received February 14, 2007



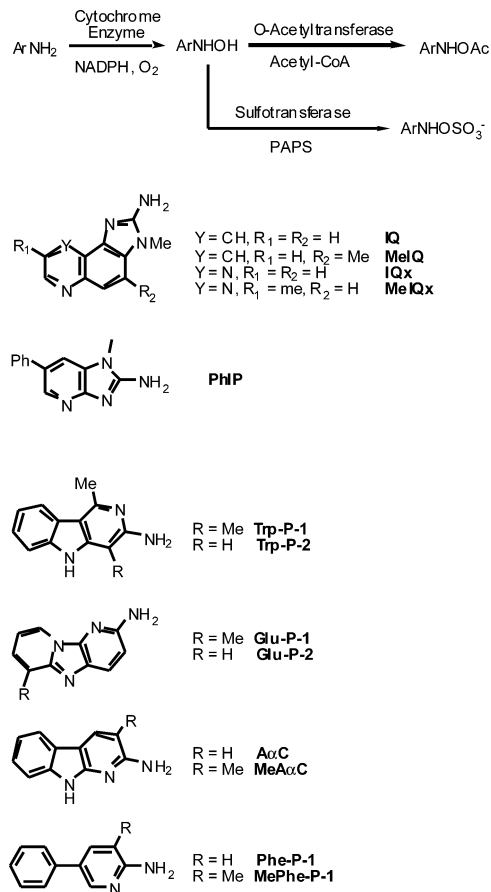
The food-derived heterocyclic amine (HCA) carcinogen 2-amino-1-methyl-6-phenyl-1*H*-imidazo[4,5-*b*]pyridine, PhIP, is often generated in the highest concentration of the HCAs formed during broiling and frying of meat and fish. Although it is considered to be an important contributor to human cancer risk from exposure to HCAs, the chemistry of PhIP metabolites that presumably react with DNA to initiate carcinogenesis has received only cursory attention. We have synthesized the ester derivative *N*-pivaloxy-2-amino-1-methyl-6-phenyl-1*H*-imidazo[4,5-*b*]pyridine, **1b**, and investigated its chemistry in aqueous solution. Although **1b** was too unstable to isolate, we could characterize it by NMR methods in DMF-*d*<sub>7</sub>, a solvent in which it is stable at  $-40\text{ }^{\circ}\text{C}$ . It decomposed rapidly in aqueous solution, but its conjugate acid, **1bH**<sup>+</sup>, is not reactive. The nitrenium ion, **2**, was trapped by N<sub>3</sub><sup>−</sup> to form the unusual tetrazole adduct, **16**. In the absence of N<sub>3</sub><sup>−</sup>, the expected hydration products of **2** were not detected, but the reduction product, **12**, was detected. Although such products are often taken as evidence of triplet nitrenium ions, the efficient trapping of **2** by N<sub>3</sub><sup>−</sup> indicates that it is a ground state singlet species. The product **12** appears to be generated by reduction of an initially formed hydration product of **2**. An alternative addition–elimination mechanism for the formation of **12** does not fit the available kinetic data. The selectivity of **2**, measured as  $k_{\text{az}}/k_{\text{s}}$ , the ratio of the second-order rate constant for its reaction with N<sub>3</sub><sup>−</sup> and the first-order rate constant for its reaction with the aqueous solvent, is  $(2.3 \pm 0.6) \times 10^4\text{ M}^{-1}$ , a value that is in the middle of the range of  $k_{\text{az}}/k_{\text{s}}$  of  $10\text{--}10^6\text{ M}^{-1}$  observed for nitrenium ions derived from other HCAs. The mutagenicity of aromatic amines (AAs) and HCAs, measured as the log of histidine revertants per nanomole of amine,  $\log m$ , in *Salmonella typhimurium* TA 98 and TA 100 correlates with  $\log(k_{\text{az}}/k_{\text{s}})$  for a wide variety of carbocyclic and heterocyclic amine mutagens including PhIP. Previously developed linear regression models for mutagenicity that include  $\log(k_{\text{az}}/k_{\text{s}})$  as an independent variable predict  $\log m$  for PhIP with good accuracy in both TA 98 and TA 100. Quantitative carcinogenicity data are less strongly correlated with  $\log(k_{\text{az}}/k_{\text{s}})$ , so prediction of the carcinogenicity of PhIP and other HCAs or AAs based primarily on  $\log(k_{\text{az}}/k_{\text{s}})$  is less successful.

Introduction

It has been known since the mid 1970s that mutagenic and carcinogenic heterocyclic amines (HCAs) are present in parts per billion concentrations in broiled and fried meats and other protein-containing foods, as well as in tobacco smoke and other

sources.<sup>1</sup> A list of selected carcinogenic HCAs is presented in Scheme 1 along with the common metabolic pathway required for activation into their ultimate carcinogenic forms, the sulfuric or acetic acid esters of the corresponding hydroxylamines.<sup>1,2</sup> The HCAs are generally classified into two structural groups:

## SCHEME 1. Structure and Metabolic Activation of Heterocyclic Amine Carcinogens



the IQ type HCAs (also called aminoimidazoazaarenes) that are characterized by an imidazoquinoline, imidazoquinoline, or imidazopyridine structure, and the non-IQ type HCAs that are characterized by a bicyclic or tricyclic ring system containing a 2-aminopyridine structure.<sup>1</sup> We have previously shown that ester derivatives of Phe-P-1, AαC, Glu-P-1, Glu-P-2, IQx, MeIQx, and Trp-P-2 decompose in aqueous solution to generate

(1) (a) Eisenbrand, G.; Tang, W. *Toxicology* **1993**, *84*, 1–82. (b) Hatch, F. T.; Knize, M. G.; Felton, J. S. *Environ. Mol. Mutagen.* **1991**, *17*, 4–19. (c) Layton, D. W.; Bogen, K. T.; Knize, M. G.; Hatch, F. T.; Johnson, V. M.; Felton, J. S. *Carcinogenesis* **1995**, *16*, 39–52. (d) Sugimura, T. *Environ. Health Perspect.* **1986**, *67*, 5–10. (f) Sugimura, T. *Mutat. Res.* **1985**, *150*, 33–41.

(2) (a) Felton, J. S.; Knize, M. G.; Shen, N. H.; Anderson, B. D.; Bjeldames, L. F.; Hatch, F. T. *Environ. Health Perspect.* **1986**, *67*, 17–24. (b) Hashimoto, Y.; Shudo, K.; Okamoto, T. *Acc. Chem. Res.* **1984**, *17*, 403–408. (c) Shinohara, A.; Saito, K.; Yamazoe, Y.; Kamataki, T.; Kato, R. *Cancer Res.* **1986**, *46*, 4362–4367. (d) Aoyama, T.; Gonzalez, F. J.; Gelboin, H. V. *Mol. Carcinogen.* **1989**, *2*, 192–198. (e) Snyderwine, E. G.; Wirth, P. J.; Roller, P. P.; Adamson, R. H.; Sato, S.; Thorgeirsson, S. S. *Carcinogenesis* **1988**, *9*, 411–418. (f) Meerman, J. H. N.; Ringer, D. P.; Coughtrie, M. W. H.; Bamforth, K. J.; Gilissen, R. A. H. *J. Chem.-Biol. Interact.* **1994**, *92*, 321–328. (g) Raza, H.; King, R. S.; Squires, R. B.; Guengerich, F. P.; Miller, D. W.; Freeman, J. P.; Lang, N. P.; Kadlubar, F. F. *Drug Metab. Dispos.* **1996**, *24*, 385–400. (h) Watanabe, M.; Ishidate, M.; Nobmi, T. *Mutat. Res.* **1990**, *234*, 337–348. (i) Turesky, R. J.; Bracco-Hammer, I.; Markovic, J.; Richli, U.; Kappeler, A.-M.; Welti, D. H. *Chem. Res. Toxicol.* **1990**, *3*, 524–535. (j) Turesky, R. J.; Markovic, J.; Bracco-Hammer, I.; Fay, L. B. *Carcinogenesis* **1991**, *12*, 1847–1855. (k) Rich, K. J.; Murray, B. P.; Lewis, I.; Rendell, N. B.; Davies, D. S.; Gooderham, N. J.; Boobis, A. R. *Carcinogenesis* **1992**, *13*, 2221–2226. (l) Snyderwine, E. G.; Schut, H. A. J.; Adamson, R. H.; Thorgeirsson, U. P.; Thorgeirsson, S. S. *Cancer Res.* **1992**, *52* (Suppl.) 2099s–2102s. (m) Schut, H. A. J.; Snyderwine, E. G. *Carcinogenesis* **1999**, *20*, 353–368.

heterocyclic nitrenium ions with N<sub>3</sub><sup>-</sup>/solvent selectivity, measured as  $k_{az}/k_s$ , the ratio of the second-order rate constant for N<sub>3</sub><sup>-</sup> trapping of the nitrenium ion and the pseudo-first-order rate constant for trapping the ion by the aqueous solvent, ranging from ca. 10 to 10<sup>6</sup> M<sup>-1</sup>.<sup>3–7</sup> We have also demonstrated that the log of the mutagenicities (log *m*) of HCAs and aromatic amines (AAs) in *Salmonella typhimurium* TA 98 and TA 100 correlate with log( $k_{az}/k_s$ ), and that two and three parameter linear regression models that include log( $k_{az}/k_s$ ) as an independent variable (significant at the 95% confidence level for log( $k_{az}/k_s$ )) predict log *m* for both *Salmonella* strains with  $r^2_{adj}$  in the range of 0.85–0.90.<sup>8</sup>

PhIP was first isolated, but not identified, from a model system containing creatinine, glucose, and glycine in 1984 by Sugimura and co-workers.<sup>9</sup> Subsequently, it was isolated and identified by Felton and co-workers in 1986 in fried ground beef.<sup>10</sup> Later studies showed that PhIP is also present in beer, wine, and cigarette smoke condensate.<sup>11,12</sup> Recent studies indicate that PhIP–DNA adducts are present in exfoliated ductal epithelial cells in human breast milk, and that PhIP itself is present in human breast milk.<sup>13,14</sup> Quantitative studies show that PhIP is usually present in the greatest concentration of the HCAs detected in cooked meat products.<sup>15–17</sup> Its mutagenicity to *Salmonella* is less than that of other IQ type HCAs and several of the other non-IQ type HCAs, including Glu-P-1, Trp-P-1, and Trp-P-2, but significantly greater than that of AAs.<sup>17</sup> Based on its relative abundance in cooked meat products and its substantial carcinogenicity in mammals, PhIP is considered to be a significant contributor to human cancer risk from HCA exposure.<sup>18</sup>

A synthetic acetic acid ester derivative of the hydroxylamine metabolite of PhIP, **1a**, apparently generates the nitrenium ion, **2**, that reacts with 2'-deoxyguanosine (d-G) residues in DNA

(3) Novak, M.; Xu, L.; Wolf, R. A. *J. Am. Chem. Soc.* **1998**, *120*, 1643–1644.

(4) Novak, M.; Kazerani, S. *J. Am. Chem. Soc.* **2000**, *122*, 3606–3616.

(5) Novak, M.; Toth, K.; Rajagopal, S.; Brooks, M.; Hott, L. L.; Moslener, M. *J. Am. Chem. Soc.* **2002**, *124*, 7972–2981.

(6) Novak, M.; Nguyen, T.-M. *J. Org. Chem.* **2003**, *68*, 9875–9881.

(7) Rajagopal, S.; Brooks, M. E.; Nguyen, T.-M.; Novak, M. *Tetrahedron* **2003**, *59*, 8003–8010.

(8) Novak, M.; Rajagopal, S. *Chem. Res. Toxicol.* **2002**, *15*, 1495–1503.

(9) Negishi, C.; Wakabayashi, K.; Tsuda, M.; Sato, S.; Sugimura, T.; Saito, H.; Maeda, M.; Jagerstad, M. *Mutat. Res.* **1984**, *140*, 55–59.

(10) Felton, J. S.; Knize, M. G.; Shen, N. H.; Lewis, P. R.; Andreson, B. D.; Happe, J.; Hatch, F. T. *Carcinogenesis* **1986**, *7*, 1081–1086.

(11) Manabe, S.; Tohyama, K.; Wada, O.; Aramaki, T. *Carcinogenesis* **1991**, *12*, 1945–1947.

(12) Manabe, S.; Suzuki, H.; Wada, O.; Ueki, A. *Carcinogenesis* **1993**, *14*, 899–901.

(13) Gorlewska-Roberts, K.; Green, B.; Fares, M.; Ambrosone, C. B.; Kadlubar, F. F. *Environ. Mol. Mutagen.* **2002**, *39*, 184–192.

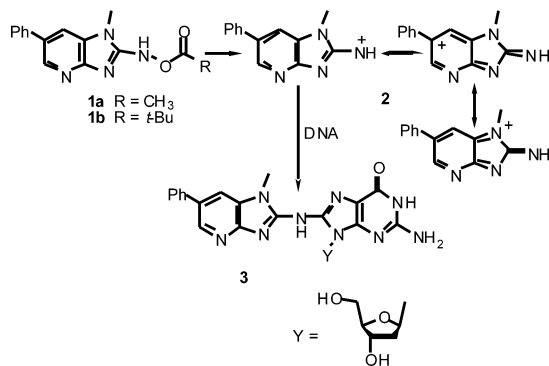
(14) (a) Thompson, P. A.; DeMarini, D. M.; Kadlubar, F. F.; McClure, G. Y.; Brooks, L. R.; Green, B. L.; Fares, M. Y.; Stone, A.; Josephy, P. D.; Ambrosone, C. B. *Environ. Mol. Mutagen.* **2002**, *39*, 134–142. (b) DeBruin, L. S.; Martos, P. A.; Josephy, P. D. *Chem. Res. Toxicol.* **2001**, *14*, 1523–1528.

(15) (a) Becher, G.; Knize, M. G.; Nes, I.; Felton, J. *Carcinogenesis* **1988**, *9*, 247–253. (b) Felton, J. S.; Knize, M. G. *Mutat. Res.* **1991**, *259*, 205–217.

(16) Skog, K. *Food Chem. Toxicol.* **1993**, *31*, 655–675.

(17) Wakabayashi, K.; Nagao, M.; Esumi, H.; Sugimura, T. *Cancer Res.* **1992**, *52* (Suppl.), 2092s–2098s.

(18) (a) Ito, N.; Hasegawa, R.; Sano, M.; Tamano, S.; Esumi, H.; Takayama, S.; Sugimura, T. *Carcinogenesis* **1991**, *12*, 1503–1506. (b) Malfatti, M. A.; Kulp, K. S.; Knize, M. G.; Davis, C.; Massengill, J. P.; Williams, S.; Nowell, S.; MacLeod, S.; Dingley, K. H.; Turtletaub, K. W.; Lang, N. B.; Felton, J. S. *Carcinogenesis* **1999**, *20*, 705–713.

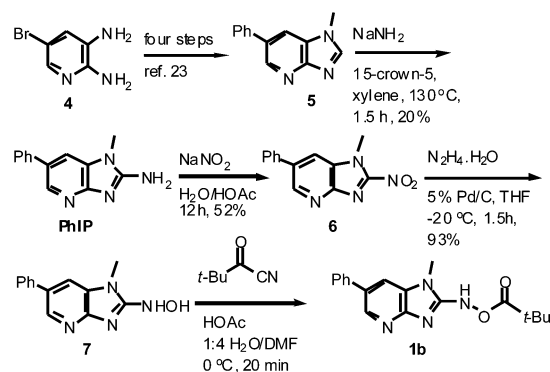
**SCHEME 2. Proposed Reaction Pathway for Generation of the PhIP-d-G Adduct in DNA**


to generate the C-8 adduct, **3** (Scheme 2).<sup>19</sup> The same adduct is detected in rats treated with PhIP.<sup>19</sup> The C-8 adduct is a characteristic product of the reaction of both carbocyclic and heterocyclic nitrenium ions with d-G,<sup>4,5,20,21</sup> but no additional characterization of **2** was performed and the ester **1a** was only characterized by mass spectrometry.<sup>19</sup> It was not known how selectively **2** reacted in an aqueous environment or whether its reactivity/selectivity correlated with the mutagenicity of PhIP. The identity of products from reaction of **2** with simple nucleophiles such as  $\text{N}_3^-$  was unknown. Typically, nucleophilic attack of  $\text{N}_3^-$  on a trigonal CH that bears a positive charge in one of the nitrenium ion resonance structures, followed by tautomerization, leads to a simple aryl azide.<sup>3-7,20,22</sup> There is no obvious way for **2** to yield such a product. Considering the abundance of PhIP in cooked meat products and its apparent importance as a human carcinogen, greater knowledge of the reactions of **1** and **2** would be advantageous.

In this paper, we present the synthesis and characterization of the pivalic acid ester, **1b**, and the characterization of its reactions in aqueous media. The pivalic acid ester was chosen because of the known tendency of acetic acid esters of some of the hydroxylamine derivatives of HCAs to undergo acyl transfer reactions rather than N–O bond cleavage.<sup>6,7</sup> Although **1b** decomposes upon attempted isolation, it is readily characterized in DMF solution and the kinetics of its decomposition are easily measured by UV methods. The reaction kinetics, reaction products, and nitrenium ion selectivity measured by  $\text{N}_3^-$ -trapping methods are described herein. The correlation of nitrenium ion selectivity with the mutagenicity and carcinogenicity of PhIP is also examined.

**Results**

The critical steps in the synthesis of **1b** are shown in Scheme 3. The four-step synthesis of **5** from **4** followed the procedures of Grivas and Lindström.<sup>23</sup> The Chichibabin reaction of **5** with excess  $\text{NaNH}_2$  in xylene at 130 °C was reported to generate PhIP in 90% yield.<sup>24</sup> We were unable to reproduce this result.

**SCHEME 3. Synthesis of 1b**


No product was detected, and **5** decomposed into a tarry residue during the reaction. Addition of 15-crown-5 to the reaction mixture, restriction of  $\text{NaNH}_2$  to a 2-fold excess over **5**, and limitation of the reaction time to 1.5 h resulted in a 20% yield of PhIP based on recovered unreacted **5**. The heterogeneous Chichibabin reaction is known to be very sensitive to the  $\text{pK}_a$  of the conjugate acid of the heterocycle undergoing amination. Typically, the reaction works only for heterocycles with  $\text{pK}_a$  values in the narrow range of 5–8.<sup>25</sup> Since the  $\text{pK}_a$  of the conjugate acid of **5** is expected to be <4.0, it is not surprising that the original procedure failed.<sup>26</sup> Addition of the crown ether brings some of the  $\text{NaNH}_2$  into solution, and the homogeneous Chichibabin reaction is known to be far less sensitive to the  $\text{pK}_a$  of the heterocycle.<sup>25</sup> The nitro compound, **6**, was generated by treatment of PhIP with excess  $\text{NaNO}_2$  in  $\text{HOAc}/\text{H}_2\text{O}$  using an adaptation of a procedure of Tanga and co-workers.<sup>27</sup> Reduction of **6** to generate the hydroxylamine, **7**, was accomplished with  $\text{N}_2\text{H}_4 \cdot \text{H}_2\text{O}$  and Pd/C using a procedure developed in our laboratory.<sup>28</sup> Due to rapid decomposition, the hydroxylamine was stored at –40 °C no longer than 24 h before conversion to **1b**. The procedure for the generation of **1b** was adapted from that previously used to generate **1a**.<sup>19</sup> Attempts to isolate and purify **1b** were unsuccessful since it rapidly decomposes upon evaporation of DMF and also decomposes on contact with silica gel. HPLC analysis of the DMF solution of **1b** generated from the synthetic procedure showed that only one major peak was present (ca. 99% by peak area). DMF solutions of **1b** were stable at –40 °C for several months but did decompose within 24–48 h at room temperature. The compound was characterized by NMR methods by performing the synthesis in  $\text{DMF-}d_7$  and collecting all NMR data at –20 °C. NMR data and details of all synthetic procedures are presented in the Supporting Information.

The decomposition kinetics of **1b** were monitored at 20 °C by UV spectroscopy. All kinetics were performed in 5 vol %  $\text{CH}_3\text{CN}-\text{H}_2\text{O}$ ,  $\mu = 0.5$  ( $\text{NaClO}_4$ ). Buffers used to maintain pH were  $\text{NaH}_2\text{PO}_4/\text{Na}_2\text{HPO}_4$ ,  $\text{AcOH}/\text{NaOAc}$ , and  $\text{HCO}_2\text{H}/\text{NaHCO}_2$  at  $\text{pH} > 2.5$ , and  $\text{HClO}_4$  solutions at  $\text{pH} \leq 2.5$ . Repetitive wavelength scans were collected for at least 5 half-lives of the decomposition reaction in the pH range of 0.5–7. The data shown in Figure 1 are typical. Isosbestic points held throughout the course of the reaction, indicating that there is no buildup of

(19) Frandsen, H.; Grivas, S.; Anderson, R.; Andersson, R.; Dragsted, L.; Larsen, J. C. *Carcinogenesis* **1992**, *13*, 629–635.

(20) Novak, M.; Rajagopal, S.; Xu, L.; Kazerani, S.; Toth, K.; Brooks, M.; Nguyen, T.-M. *J. Phys. Org. Chem.* **2004**, *17*, 615–624.

(21) Novak, M.; Kennedy, S. A. *J. Am. Chem. Soc.* **1995**, *117*, 574–575.

(22) Novak, M.; Kahley, M. J.; Eiger, E.; Helmick, J. S.; Peters, H. E. *J. Am. Chem. Soc.* **1993**, *115*, 9453–9460.

(23) Grivas, S.; Lindstrom, S. *J. Heterocycl. Chem.* **1995**, *32*, 467–471.

(24) Choshi, T.; Tonari, A.; Yoshioka, H.; Harada, K.; Sugino, E.; Hibino, S. *J. Org. Chem.* **1993**, *58*, 7952–7954.

(25) McGill, C. K.; Rappa, A. In *Advances in Heterocyclic Chemistry*; Katritzky, A. R., Ed.; Academic Press: San Diego, 1988; Vol. 44, pp 1–79.

(26) Perrin, D. D. *J. Chem. Soc.* **1965**, 5590–5596.

(27) Tanga, M. J.; Bupp, J. E.; Bradford, W. W. *J. Labelled Compd. Radiopharm.* **2001**, *44*, 405–411.

(28) Kazerani, S.; Novak, M. *J. Org. Chem.* **1998**, *63*, 895–897.

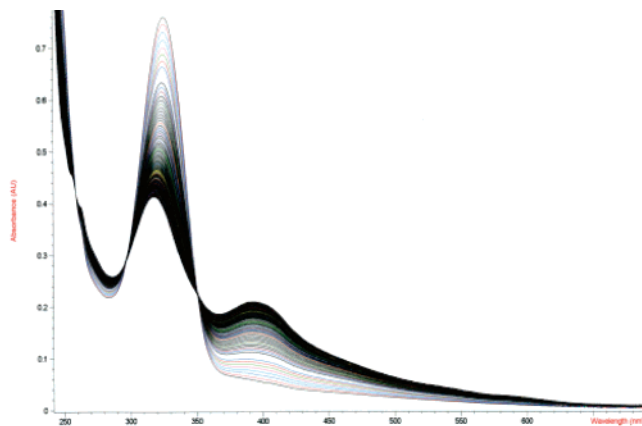


**FIGURE 1.** Repetitive wavelength scans for **1b** at pH 6.81, in 0.02 M  $\text{NaH}_2\text{PO}_4/\text{Na}_2\text{HPO}_4$  buffer at 20 °C, total time = 10 min, cycle time = 5 s.

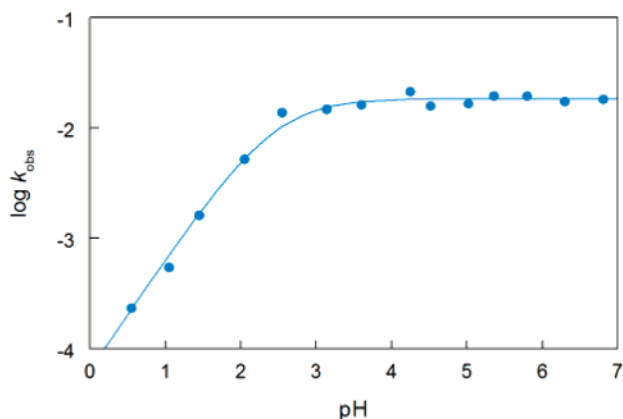


**FIGURE 2.** Log  $k_{\text{obs}}$  versus pH for **1b**. Data were fit to eq 1.

a detectable intermediate during the decomposition of **1b** over this pH range. In some solutions, precipitation occurred, but only after at least 5 half-lives of the reaction. This did not interfere with determination of rate constants. Absorbance versus time data collected at 325 nm fit the first-order rate equation well at all pH. Pseudo-first-order rate constants were determined from the average of duplicate runs at all pH and buffer concentrations. Tables of rate constants are provided in the Supporting Information.

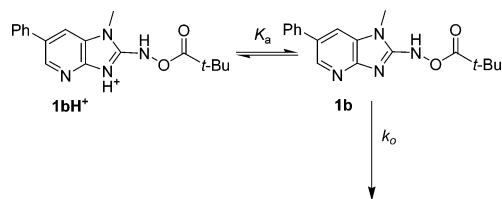
Rate constants were independent of buffer concentrations, but did exhibit pH dependence as shown in Figure 2. The rate data fit the rate law of eq 1 well.

$$k_{\text{obs}} = K_a k_o / (K_a + 10^{-\text{pH}}) \quad (1)$$

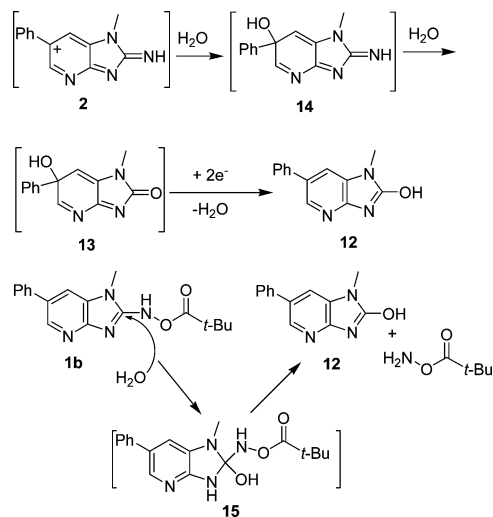
The apparent ionization constant,  $K_a$ , was also detected through spectrophotometric titration of **1b** performed by plotting initial absorbance at 325 nm versus pH (data provided in the Supporting Information). The  $\text{p}K_a$  measured from the kinetic fit ( $2.46 \pm 0.04$ ) is in good agreement with the spectrophotometrically measured  $\text{p}K_a$  ( $2.52 \pm 0.05$ ). The limiting rate constant at neutral pH,  $k_o$ , is  $(1.85 \pm 0.08) \times 10^{-2} \text{ s}^{-1}$ .

The rate law of eq 1 was previously observed for other ester derivatives of heterocyclic hydroxylamines obtained from Phe-P-1,  $\text{AcC}$ ,  $\text{IQx}$ , and  $\text{MeIQx}$ .<sup>3–5</sup> The rate law is consistent with the uncatalyzed decomposition of the conjugate base of an unreactive acid, **1bH**<sup>+</sup> (Scheme 4).<sup>3</sup> Protonation could occur at

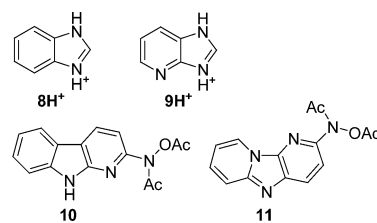
#### SCHEME 4. Kinetic Scheme Consistent with Equation 1



#### SCHEME 5. Possible Routes to 12



either N-3 or N-4 of **1b**. The  $\text{p}K_a$  trends for the conjugate acids of 1*H*-benzimidazole, **8H**<sup>+</sup> (5.53), and 1*H*-imidazo[4,5-*b*]pyridine, **9H**<sup>+</sup> (3.92), suggest that protonation of **1b** occurs at N-3.<sup>26</sup>



Substitution with the electron-withdrawing NHO pivaloxy group at C-2 and the steric hindrance to solvation caused by that bulky group account for the decreased  $\text{p}K_a$  observed for **1bH**<sup>+</sup>.<sup>4,5,29</sup> Although **1b** is protonated under acidic conditions, it is not reactive at low pH. Some conjugate acids of esters of hydroxamic acids derived from the HCAs, such as **10** and **11**, do undergo either spontaneous or acid-catalyzed decomposition, but no hydroxylamine esters derived from HCAs have exhibited observable reactivity of their conjugate acids.<sup>3–7,20</sup>

The only detectable products of the decomposition of **1b** in pH 6.8 phosphate buffer detected by HPLC were **12** ( $48 \pm 2\%$ ) and **5** ( $17 \pm 1\%$ ). Neither of these are simple hydrolysis products of **1b**, although **12** is a  $2e^-$  reduction product of the anticipated, but undetected, hydrolysis product, **13** (Scheme 5), and **5** is a  $4e^-$  reduction product of **13**. Although the source of reducing equivalents is not clear, reduction products are commonly observed among the decomposition products of hydroxylamine and hydroxamic ester derivatives of HCAs.<sup>4,6,7,20</sup> Compound **12** is the major decomposition product of **1b** upon long-term storage

(29) Novak, M.; Martin, K. A. *J. Org. Chem.* **1991**, *56*, 1585–1590.



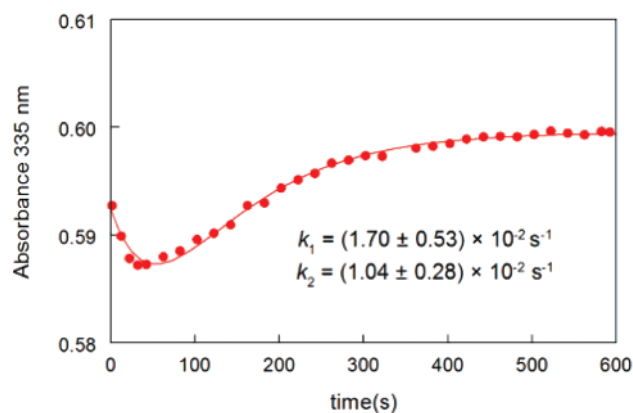


**FIGURE 3.** Absorbance at 335 nm versus time for the decomposition of **1b** in pH 6.8 phosphate buffer containing 10 mM  $N_3^-$ . Data were fit to the consecutive first-order rate equation:  $A_t = A_1 \exp(-k_1 t) + A_2 \exp(-k_2 t) + A_\infty$  by a five parameter nonlinear least-squares procedure.

in DMF solutions at  $-40^\circ\text{C}$ . It has also previously been observed as a byproduct of the formation of the nitro compound, **6**, and can be made by refluxing **6** in 2/1 DMF/ $H_2O$  for ca. 10–15 min.<sup>30,31</sup> This reaction, and the formation of PhIP from **5** via the Chichibabin reaction (above), suggests an alternative process for the formation of **12** from **1b** via an addition–elimination reaction involving the intermediate **15**. Although our solutions of **1b** in DMF do slowly decompose into **12**, we can demonstrate by NMR and HPLC methods that there is insufficient **12** present in freshly made solutions of **1b** (typically 2–5%) to account for the results of our hydrolysis product study. The precipitate encountered in some reactions appears to be polymeric and was not further characterized.

Decomposition of **1b** in pH 6.8 phosphate buffer in the presence of  $N_3^-$  leads to a number of significant changes in kinetics and products. The data in Figure 3 show that the reaction in the presence of  $N_3^-$  no longer exhibits first-order behavior but is characterized by a consecutive first-order process that is observed over the entire range of  $[N_3^-]$  examined (0.5–10 mM).

Error limits for the two rate constants obtained in each least-squares fit are relatively large as a consequence of the fact that the two rate constants differ by less than a factor of 2. The magnitudes of the rate constants are independent of  $[N_3^-]$  (Figure 4), and the standard deviations of the averages of each rate constant obtained from seven determinations are acceptably small at ca. 10%. One of the two rate constants observed under these conditions,  $k_1$ , is of the same magnitude (average value in the range of 0.5–10 mM  $N_3^-$  of  $(1.64 \pm 0.18) \times 10^{-2} \text{ s}^{-1}$ ) as  $k_{\text{obs}}$  detected in the absence of  $N_3^-$  ( $(1.78 \pm 0.08) \times 10^{-2} \text{ s}^{-1}$  at pH 6.8) (Figure 4). The other rate constant,  $k_2$ , is somewhat smaller (average value =  $(0.99 \pm 0.10) \times 10^{-2} \text{ s}^{-1}$ ) and appears to be associated with a process that only occurs in the presence of  $N_3^-$ . The data indicate that  $k_1$  is  $k_{\text{obs}}$ , the rate constant for the disappearance of **1b**, that is unaffected by the presence of  $N_3^-$ , and  $k_2$  is a rate constant that describes the decomposition of an intermediate produced by the reaction of  $N_3^-$  with the initial product of the decomposition of **1b**.

(30) Frandsen, H.; Rasmussen, E. S.; Nielsen, P. A.; Farmer, P.; Dragsted, L.; Larsen, J. C. *Mutagenesis* **1990**, *6*, 93–98.

(31) (a) Alexander, J.; Wallin, H.; Rosslund, O. J.; Solberg, K. E.; Holme, J. A.; Becher, G.; Andersson, R.; Grivas, S. *Carcinogenesis* **1991**, *12*, 2239–2245. (b) Crofts, F. G.; Strickland, P. T.; Hayes, C. L.; Sutter, T. R. *Carcinogenesis* **1997**, *18*, 1793–1798.

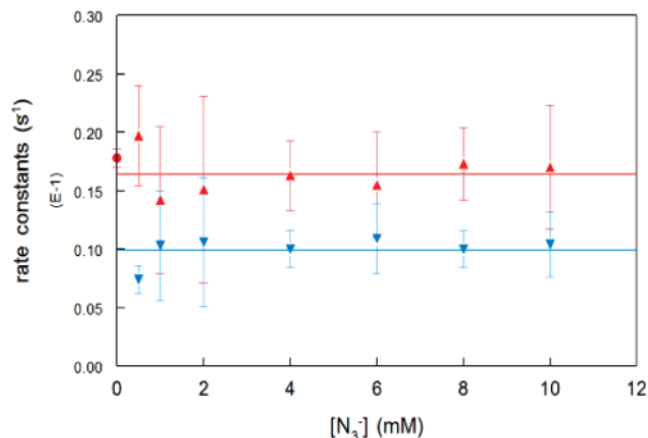
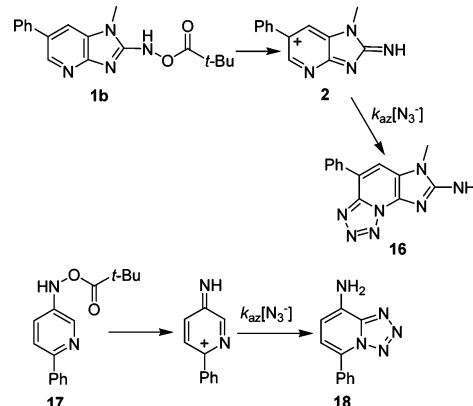


**FIGURE 4.** Comparison of  $k_1$  and  $k_2$  measured during the decomposition of **1b** in the presence of  $N_3^-$  with  $k_{\text{obs}}$  measured in the absence of  $N_3^-$ :  $k_{\text{obs}}$  (●),  $k_1$  (▲),  $k_2$  (▼). Average values of  $k_1$  and  $k_2$  are indicated by the red and blue lines, respectively.

#### SCHEME 6. Tetrazole Products from **1b** and **17**



Product studies showed that at  $[N_3^-] \geq 1 \text{ mM}$ , one new reaction product, **16**, is generated in quantitative yield (Scheme 6). No other products are detected under these conditions. The tetrazole structure of **16** is unusual for an azide adduct of a heterocyclic hydroxylamine or hydroxamic acid ester, but not unprecedented. The ester **17** yields the tetrazole **18** in the presence of  $N_3^-$ .<sup>3</sup> At  $[N_3^-] \leq 0.5 \text{ mM}$ , the yield of **16** becomes dependent on  $[N_3^-]$ . The rate and product yield data are consistent with trapping of an intermediate cation generated by rate-limiting ionization. The data (Figure 5) are fit well by eq 2.

$$[\mathbf{15}] = [\mathbf{15}]_{\text{max}} \left( \frac{k_{\text{az}}[N_3^-]/k_s}{1 + k_{\text{az}}[N_3^-]/k_s} \right) \quad (2)$$

In eq 2, the azide/solvent trapping ratio,  $k_{\text{az}}/k_s$ , is the ratio of the second-order rate constant for trapping of **2** by  $N_3^-$  ( $k_{\text{az}}$ ) and the putative first-order rate constant for trapping by the aqueous solvent ( $k_s$ ). This equation is commonly used to characterize the yield of the  $N_3^-$ -trapping products for heterocyclic and carbocyclic nitrenium ions and carbenium ions.<sup>3–7,22,32</sup> The azide/solvent trapping ratio,  $k_{\text{az}}/k_s$ , for **2** of  $(2.3 \pm 0.6) \times 10^4 \text{ M}^{-1}$  is of intermediate magnitude compared to that of other heterocyclic nitrenium ions.<sup>3–7,20</sup>

(32) (a) Richard, J. P.; Jencks, W. P. *J. Am. Chem. Soc.* **1982**, *104*, 4689–4691; **1982**, *104*, 4691–4692; **1984**, *106*, 1383–1396. (b) Richard, J. P.; Amyes, T. L.; Vontor, T. *J. Am. Chem. Soc.* **1991**, *113*, 5871–5873.

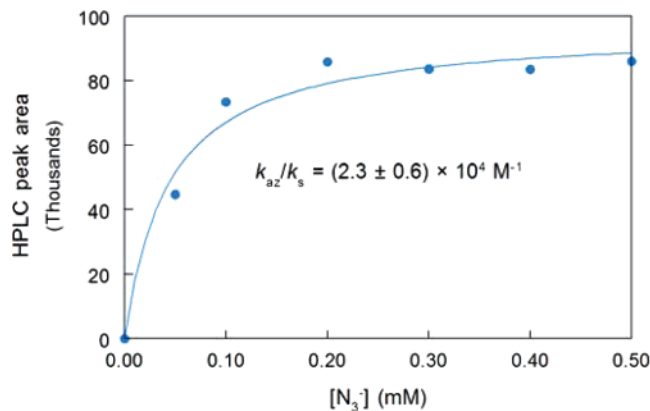


FIGURE 5. Yield of **16** as a function of  $[N_3^-]$ . Data were fit to eq 2.

Quantitative structure–activity relationships, QSARs, are used to correlate quantitative bacterial mutagenicity data and carcinogenicity data for both AAs and HCAs with calculated or observed properties of the amines or the corresponding nitrenium ions.<sup>33</sup> The dependent variable in most of the mutagenicity correlations is the logarithm of histidine revertants in *Salmonella typhimurium* strains TA 98 or TA 100 per nanomole of amine ( $\log m$ ) taken under conditions in which the S-9 fraction of rat liver homogenates, induced by Arachlor 1254 or other PCB preparations, is added to the preparation.<sup>33,34</sup> We recently showed that  $\log m$  for both *Salmonella* strains for a set of 18 AAs and HCAs with widely varying structure correlated with  $\log S$ , the log of the experimental azide/solvent product ratio at 1 M  $N_3^-$  for the corresponding nitrenium ions ( $r_{\text{adj}}^2 = 0.5491$  for TA 98 and 0.6338 for TA 100).<sup>8</sup>  $\log S$  is equivalent to  $\log(k_{\text{az}}/k_s)$  for nitrenium ions with  $\log S \geq 1$ .<sup>8</sup> We developed two parameter linear regression models, significant at the 95% confidence level for both variables, that included  $\log S$  and a ring index variable,  $I_{\text{rings}}$ , that is 0 for monocyclic AAs (MAAs) and 1 for all other amines ( $r_{\text{adj}}^2 = 0.8448$  for TA 98 and 0.8927 for TA 100). Inclusion of a third variable,  $C \log P$ , increased  $r_{\text{adj}}^2$  to 0.8913 for TA 98 and 0.9011 for TA 100, but the model is only significant at the 80% confidence level for  $C \log P$  in TA 100.<sup>8</sup>

Figure 6 shows that the  $\log m$  versus  $\log S$  data for PhIP appear to be unremarkable when compared to the same data for the amines included in our previous correlation.  $\log m$  for PhIP for both strains of *Salmonella* is found in the literature,<sup>17</sup> while  $\log(k_{\text{az}}/k_s)$  ( $\log S$ ) is from the current study. The regression lines for both *Salmonella* strains are shown with and without the inclusion of the PhIP data. The significantly smaller mutagenicity of MAAs compared to polycyclic amines with nitrenium ions of similar  $\log S$  was previously noted and is the reason for the inclusion of  $I_{\text{rings}}$  in the regression models.<sup>8</sup>

(33) (a) Benigni, R.; Giuliani, A.; Franke, R.; Gruska, A. *Chem. Rev.* **2000**, *100*, 3697–3714. (b) Colvin, M. E.; Hatch, F. T.; Felton, J. S. *Mutat. Res.* **1998**, *400*, 479–492. (c) Chung, K.-T.; Kirkovsky, L.; Kirkovsky, A.; Purcell, W. P. *Mutat. Res.* **1997**, *387*, 1–16.

(34) (a) Maron, D. M.; Ames, B. N. *Mutat. Res.* **1983**, *113*, 173–215. (b) Debnath, A. K.; Debnath, G.; Shusterman, A. J.; Hansch, C. *Environ. Mol. Mutagen.* **1992**, *19*, 37–52. (c) Hatch, F. T.; Knize, M. G.; Felton, J. S. *Environ. Mol. Mutagen.* **1991**, *17*, 4–19. (d) Hatch, F. T.; Colvin, M. E.; Seidl, E. T. *Environ. Mol. Mutagen.* **1996**, *27*, 314–330. (e) Hatch, F. T.; Colvin, M. E. *Mutat. Res.* **1997**, *376*, 87–96. (f) Hatch, F. T.; Knize, M. G.; Colvin, M. E. *Environ. Mol. Mutagen.* **2001**, *38*, 268–291. (g) Maran, U.; Karelson, M.; Katritzky, A. R. *Quant. Struct.-Act. Relat.* **1999**, *18*, 3–10.

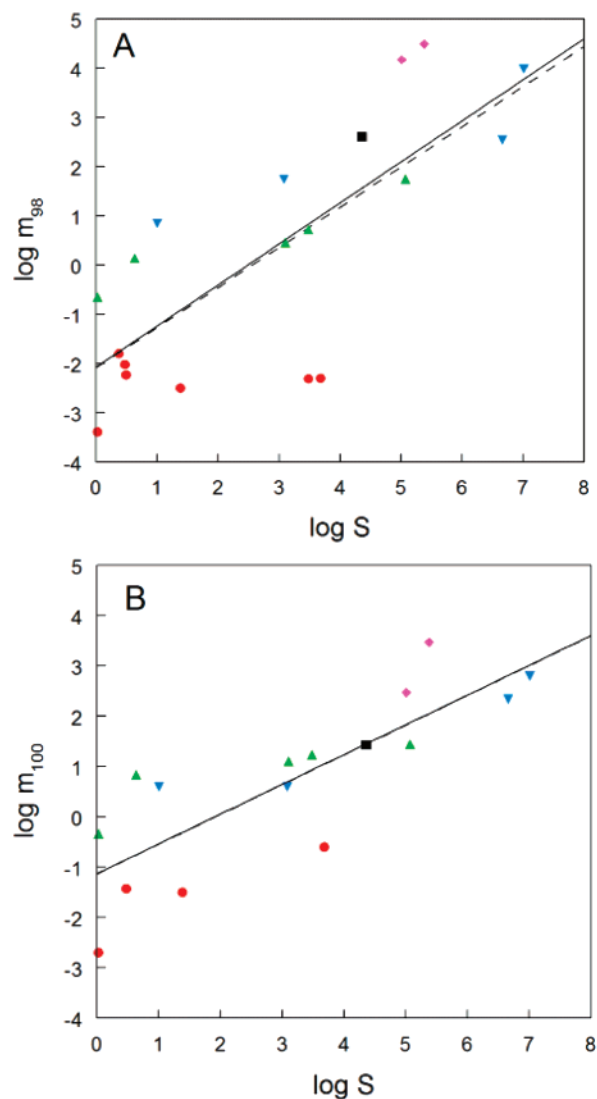
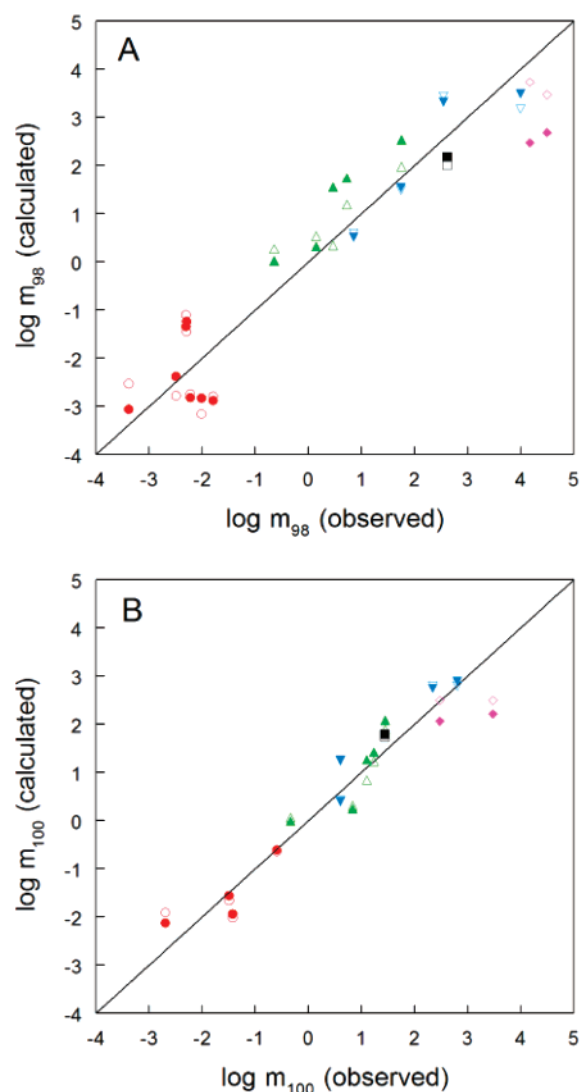


FIGURE 6.  $\log m$  for  $ArNH_2$  expressed as  $\log(\text{revertants/nmol})$  versus  $\log S$  for  $ArNH_2^+$  for *S. typhimurium* TA 98 (A) and TA 100 (B): IQ type HCAs ( $\blacklozenge$ , magenta), non-IQ type HCAs ( $\blacktriangledown$ , blue), PAAs ( $\blacktriangle$ , green), MAAs ( $\bullet$ , red), and PhIP ( $\blacksquare$ , black). All data except PhIP are from ref 8. PhIP data are from ref 17 and this work. Dashed lines are least-squares regression lines excluding PhIP ( $r_{\text{adj}}^2 = 0.5491$  for TA 98, 0.6338 for TA 100); solid lines are the least-squares regression lines for the entire data set ( $r_{\text{adj}}^2 = 0.5614$  for TA 98, 0.6400 for TA 100). The two lines nearly superimpose for TA 100.

In Figure 7, the values of  $\log m$  calculated from the regression models are plotted against the experimental  $\log m$  for the amines in the previous study and for PhIP. The regression model equations for both *Salmonella* strains were not recalculated for the PhIP data. Instead, the calculated  $\log m$  for PhIP was obtained from the previously determined regression equations. The data for PhIP clearly fall into the trend observed for the AAs and other HCAs.

## Discussion

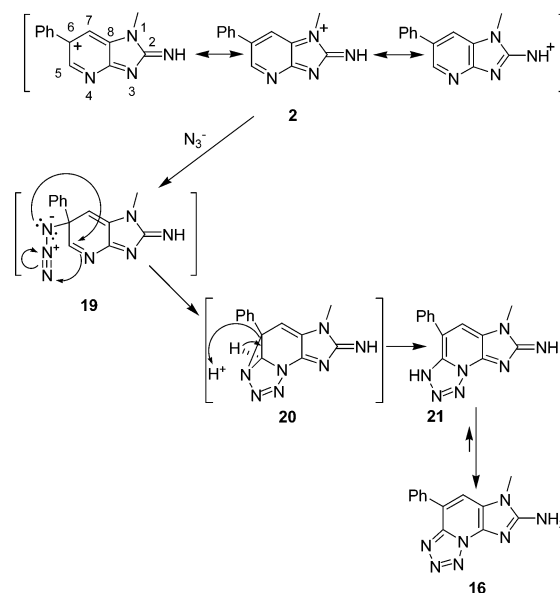
Although **1b** could not be isolated, it is clear from the NMR characterization in  $DMF-d_7$  and the observed reactions that this compound was generated. The previously reported synthesis of **1a** appears to be verified since it was made by an analogous method from the hydroxylamine, **7**.<sup>19</sup> The pH rate profile for



**FIGURE 7.** Plots of calculated versus observed  $\log m$  for TA 98 (A) and TA 100 (B) for the two variable ( $\log S$  and  $I_{\text{rings}}$ ) regression model of ref 8 (closed symbols) and the three variable ( $\log S$ ,  $I_{\text{rings}}$ , and  $C \log P$ ) regression model of ref 8 (open symbols). Symbols are defined in Figure 6. The models were not recalculated for PhIP. The calculated values of  $\log m$  for PhIP were determined from the previously calculated regression equations, and the observed  $\log m$  values were obtained from ref 17.

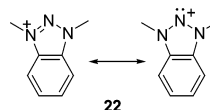
**1b** (Figure 2) explains the greater stability of **1a** that was observed under acidic conditions.<sup>19</sup> The  $\text{N}_3^-$ -trapping kinetics results indicate that trapping occurs on an intermediate generated after the rate-limiting reaction step. Direct  $\text{N}_3^-$  attack on **1b** is ruled out because of the lack of dependence of the rate of decomposition of **1b** on  $[\text{N}_3^-]$  (Figure 4). The most likely intermediate is the nitrenium ion, **2**. The C-8 adduct, **3**, reported from reaction of **1a** with DNA is also likely to be generated by reaction with **2** based on the trapping results for **1b** and those we previously reported for the reaction of heterocyclic nitrenium ions with d-G.<sup>4,5,19,20</sup> The overall similarity in reaction kinetics and trapping results with those of other ester derivatives of heterocyclic hydroxylamines that have been demonstrated to yield nitrenium ions also supports our conclusion.<sup>3–5</sup> Unlike other nitrenium ions that we have investigated, **2** cannot form a stable aromatic  $\text{N}_3^-$  adduct by tautomerization of an initially formed adduct because the carbon atoms in **2** that bear a positive

#### SCHEME 7. Possible Mechanism for the Formation of **16**



charge are  $4^\circ$  (C-6 and C-8, Scheme 7). An intriguing possibility for the formation of the observed tetrazole product, **16**, is initial attack on C-6 to form **19**, followed by an intramolecular dipolar cycloaddition to form **20**. Aziridine ring opening with elimination of the C-5 proton leads to **21**, a tautomer of **16**. Either **20** or **21** could be the intermediate responsible for the rate constant  $k_2$  detected during the trapping experiments. An alternative mechanism involving attack of  $\text{N}_3^-$  on pyridyl N-4 followed by cyclization to C-5 coupled with net proton transfer from C-5 to the exocyclic N cannot be ruled out by the available data. This mechanism is considered less likely because  $\text{N}_3^-$  always attacks C rather than N in other heterocyclic and carbocyclic nitrenium ions.<sup>3–7,22</sup>

The dipolar cycloaddition of alkyl azides with nitriles to form tetrazoles is well-known.<sup>35</sup> Alkyl azides also react with isocyanates to form tetrazolones.<sup>36</sup> Dipolar cycloadditions of alkyl azides with simple imines appear not to have been reported, but the proposed intramolecular cycloaddition would be entropically favored. Aziridine ring opening reactions are quite common, but formation of a detectable enamine product as in **21** is rare.<sup>37</sup> Aromatization of the system may provide sufficient driving force to bring about this conversion.



The origin of the unusual reaction product **12** and the minor product **5** is of interest. As shown in Scheme 5, these products cannot be obtained from the nitrenium ion **2** without a reduction

(35) (a) Smith, P. A. S.; Clegg, J. M.; Hall, J. H. *J. Org. Chem.* **1958**, *23*, 524–529. (b) Carpenter, W. R. *J. Org. Chem.* **1962**, *27*, 2085–2088. (c) Kay, D. P.; Kennewell, P. D.; Westwood, R. *J. Chem. Soc., Perkin Trans. 1* **1982**, 1879–1884. (d) Klaubert, D. H.; Bell, S. C.; Pattison, T. W. *J. Heterocycl. Chem.* **1985**, *22*, 333–336. (e) Demko, Z. P.; Sharpless, K. B. *Angew. Chem., Int. Ed.* **2002**, *41*, 2113–2116.

(36) (a) Chung, J. Y. L.; Ho, G.-J.; Chartrain, M.; Roberge, C.; Zhao, D.; Leazer, J.; Farr, R.; Robbins, M.; Emerson, K.; Mathre, D. J.; McNamara, J. M.; Hughes, D. L.; Grabowski, E. J. J.; Reider, P. J. *Tetrahedron Lett.* **1999**, *40*, 6739–6743. (b) Denecker, G.; Smets, G.; L'Abbe, G. *Tetrahedron* **1975**, *31*, 765–775.

(37) Bellos, K.; Stamm, H. *J. Org. Chem.* **1995**, *60*, 5661–5666.

process. Reduction and dimerization products often dominate the chemistry of other heterocyclic nitrenium ions, and the sources of reducing equivalents are difficult to determine.<sup>20</sup> The suspected sources of reducing equivalents in many cases are the initial hydration products.<sup>4,20</sup> If **13** or **14** were the source of reduction equivalents, oxidation products of **13** or **14** would be expected. None were detected, but the combined yield of **12** and **5** is less than quantitative (ca. 65%), so there is a significant amount of undetected reaction product. Reduction products observed during the triplet sensitized photolysis of certain carbocyclic nitrenium ion precursors have been taken as evidence for the presence of triplet state nitrenium ions.<sup>38</sup> Experimental and theoretical results suggest that carbocyclic nitrenium ions with low energy triplet states that might be accessible during thermal generation are highly unstable short-lived species that are difficult to trap with nucleophilic trapping agents.<sup>38,39</sup> That is not the case for heterocyclic nitrenium ions that generate reduction products. They are always species of moderate to high azide/solvent selectivity that can be quantitatively trapped by  $N_3^-$  or other nucleophiles.<sup>3-7,20</sup> A limited number of calculations on heterocyclic nitrenium ion singlet-triplet gaps have appeared, and the singlet-triplet gap for one highly stabilized heterocyclic nitrenium ion has been experimentally measured.<sup>40-42</sup> The persistent 1,3-dimethylbenzotriazolium ion, **22**, is a ground state singlet with a singlet-triplet gap of  $-(66 \pm 3)$  kcal/mol.<sup>40</sup> The calculations indicate that heteroatoms positioned to generate closed shell resonance structures, such as N-1 in **2** or N-1 and N-3 in **22**, stabilize the singlet electronic state preferentially, while heteroatoms positioned to bear a positive charge without generation of a closed shell resonance structure, such as N-3 and N-4 of **2**, preferentially destabilize the singlet state.<sup>40-42</sup> The available experimental data and the calculations suggest that **2** is unlikely to have an accessible triplet state.

An alternative explanation of the origin of **12** is that it is formed via an addition-elimination mechanism that does not involve **2** (Scheme 5). This attractive proposal has precedent in the chemistry of this system, but it is at odds with the available experimental evidence. At 20 °C the half-life of **1b** in aqueous solution is only 37 s. Compound **6** that has a considerably better leaving group ( $NO_2^-$ ) than **1b** is stable in aqueous solution at room temperature for several days. It must be refluxed in DMF/H<sub>2</sub>O mixtures to be converted into **12**.<sup>30,31</sup> The pH dependence of the decomposition of **1b** is difficult to reconcile with this proposal. Protonation of **1b** would be expected to activate it toward nucleophilic substitution via the addition-elimination mechanism, but experimentally, **1b** is stabilized by protonation. Finally, the results of  $N_3^-$  trapping are inconsistent with this proposal. Trapping by  $N_3^-$  occurs quantitatively at  $[N_3^-] \geq 1$  mM without rate acceleration. This could not occur if **12** was generated by a competing addition-elimination process unless the formation of the nitrenium ion, **2**, was reversible, and almost all of the nitrenium ion returned to **1b** in the absence of  $N_3^-$ . This is highly unlikely at the

concentrations of pivalate ion that must be present under the reaction conditions ( $\leq 2.5 \times 10^{-5}$  M) for an ion that has moderate stability in aqueous solution and is in diffusional equilibrium with nonsolvent nucleophiles based on the  $N_3^-$ -trapping data.<sup>43</sup> Addition-elimination chemistry might be possible for **1b** in a solvent that does not favor ionization, but in aqueous solution, ionization apparently overwhelms other possible pathways. We intend to examine this possibility at a future date.

Since our analysis indicates that **12** is ultimately generated from the cation **2**, the rate constant ratio determined by the  $N_3^-$ -trapping experiments does appear to be  $k_{az}/k_s$  for that ion. Rate constants for the reaction of  $N_3^-$  with moderately selective nitrenium ions ( $k_{az}/k_s \leq 10^5$  M<sup>-1</sup>) occur at the diffusion-controlled limit of ca.  $5 \times 10^9$  M<sup>-1</sup> s<sup>-1</sup>.<sup>44</sup> If this is true for **2**, the measured  $k_{az}/k_s$  of  $(2.3 \pm 0.6) \times 10^4$  M<sup>-1</sup> leads to an estimate of  $k_s$  for this ion of ca.  $2.2 \times 10^5$  s<sup>-1</sup> or a lifetime ( $1/k_s$ ) of  $4.6 \times 10^{-6}$  s. Since  $k_{az}/k_s$  varies from 10 to  $10^6$  M<sup>-1</sup> for a wide range of heterocyclic nitrenium ions, **2** is an ion of intermediate selectivity.<sup>3-7,20</sup> It is about as selective as the ion derived from AαC but much less selective than ions derived from IQx, MeIQx, Glu-P-1, and Glu-P-2.<sup>4,5</sup> Whatever the mechanism for the formation of **12** may be, the experimentally determined value of  $k_{az}/k_s$  does measure the selectivity for reaction of **2** with  $N_3^-$  compared to all other possible reactions in the absence of  $N_3^-$ , so it is a valid experimental measure of the selectivity of **2**.

Although **2** generates an unusual azide adduct, Figures 6 and 7 show that the overall selectivity of **2**, measured as  $\log(k_{az}/k_s)$  ( $\log S$ ), does predict the mutagenicity of PhIP in *Salmonella typhimurium* TA 98 and TA 100 based on our previously developed linear regression model for mutagenicity. That model uses  $\log(k_{az}/k_s)$  as an independent variable based on the underlying hypothesis that the nitrenium ion selectivity controls the efficiency of reaction of the nitrenium ion with DNA in vivo, and that the formation of the DNA adduct is a dominant factor in mutagenesis.<sup>8</sup> The success of the regression model suggests that the hypothesis may be correct. Since **2** is of intermediate azide/solvent selectivity compared to the variety of both carbocyclic and heterocyclic nitrenium ions previously examined, PhIP would be expected to be of intermediate mutagenicity. Figure 6 shows that is the case, and Figure 7 shows that the previously developed regression model adequately predicts the mutagenicity of PhIP in both *Salmonella* strains. The azide/solvent selectivity is less successful at correlating carcinogenicity of aromatic amines in mice and rats.<sup>8</sup> Although there is a positive correlation, carcinogenicity data, expressed as  $-\log TD_{50}$ , exhibit much less dependence on  $\log(k_{az}/k_s)$  than does  $\log m$  with considerably more scatter.<sup>8</sup> Since  $\log m$  for AAs and HCAs varies over a range of ca. 8 log units while carcinogenicity data for the same amines vary over ca. 4 log units, slopes of the correlation lines for  $-\log TD_{50}$  are about half of those for  $\log m$ . Plots of  $-\log TD_{50}$  for mice (13 amines

(38) Falvey, D. E. *J. Phys. Org. Chem.* **1999**, *12*, 589–596.

(39) (a) Sullivan, M. B.; Brown, K.; Cramer, C. J.; Truhlar, D. G. *J. Am. Chem. Soc.* **1998**, *120*, 11778–11783. (b) Winter, A. H.; Falvey, D. E.; Cramer, C. J. *J. Am. Chem. Soc.* **2004**, *126*, 9661–9668.

(40) McLlroy, S.; Cramer, C. J.; Falvey, D. E. *Org. Lett.* **2000**, *2*, 2451–2454.

(41) Sullivan, M. B.; Cramer, C. J. *J. Am. Chem. Soc.* **2000**, *122*, 5588–5596.

(42) Hilal, R.; Khalek, A. A. A.; Elroby, S. A. K. *THEOCHEM* **2005**, *731*, 115–121.

(43) A reviewer has suggested that **12** could be formed by an intramolecular rearrangement of **1b** to a spiro intermediate that undergoes hydrolytic decomposition to **12** and *O*-pivaloylhydroxylamine. This suggestion might explain the rapid reaction of **1b** but is still inconsistent with the  $N_3^-$ -trapping data.

(44) (a) Davidse, P. A.; Kahley, M. J.; McClelland, R. A.; Novak, M. J. *Am. Chem. Soc.* **1994**, *116*, 4513–4514. (b) McClelland, R. A.; Gadosy, T. A.; Ren, D. *Can. J. Chem.* **1998**, *76*, 1327–1337. (c) McClelland, R. A.; Davidse, P. A.; Hadzialic, G. *J. Am. Chem. Soc.* **1995**, *117*, 4173–4174. (d) Ren, D.; McClelland, R. A. *Can. J. Chem.* **1998**, *76*, 78–84. (e) Bose, R.; Ahmad, A. R.; Dicks A. P.; Novak, M.; Kayser, K. J.; McClelland, R. A. *J. Chem. Soc., Perkin Trans. 2* **1999**, 1591–1599.



including PhIP) and rats (11 amines including PhIP) versus log  $S$  are shown in the Supporting Information. Of the variables previously examined,  $C \log P$  provided the strongest correlation with the carcinogenicity data, in agreement with earlier observations made on a larger data set.<sup>8,33a</sup> The weaker correlation to a single variable is not surprising since carcinogenesis in mammals is a far more complicated process than mutagenesis in bacteria. In light of these correlations, it is not surprising that PhIP was demonstrated to be more effective than other HCAs, including several that are more mutagenic than PhIP, in transforming cultured mammalian cells.<sup>45</sup>

## Experimental Section

General procedures for purifying solvents, preparing solutions, measuring rate constants by UV methods, and performing product studies by HPLC have been published.<sup>22,46,47</sup> All salts used in the preparation of the buffers were reagent grade and commercially available. H<sub>2</sub>O used in the kinetics studies was distilled, deionized, and redistilled. MeOH used as an HPLC solvent was reagent grade and was distilled before use. H<sub>2</sub>O used as an HPLC solvent was distilled and deionized. Syntheses and characterization of all compounds used in this study are presented in the Supporting Information. The ester **1b** could not be isolated but was prepared in DMF solutions in which it was stable for several months if stored at  $-40\text{ }^{\circ}\text{C}$ .

**Kinetic Studies.** All kinetics were performed in 5 vol % CH<sub>3</sub>CN–H<sub>2</sub>O,  $\mu = 0.5$  (NaClO<sub>4</sub>), at 20 °C. Buffers used to maintain pH were 0.02 M NaH<sub>2</sub>PO<sub>4</sub>/Na<sub>2</sub>HPO<sub>4</sub>, 0.02 M AcOH/NaOAc, and 0.02 M HCO<sub>2</sub>H/NaHCO<sub>2</sub> at pH > 2.5, and HClO<sub>4</sub> solutions at pH  $\leq 2.5$ . Higher concentrations of buffers were used to examine the possibility of buffer catalysis. A stock solution of **1b** was prepared in DMF at a concentration of ca.  $5 \times 10^{-3}$  M as described in the Supporting Information. Injection of 15  $\mu\text{L}$  of this stock solution into 3.0 mL of buffer at 20 °C generated reaction solutions of initial concentration of ca.  $2.5 \times 10^{-5}$  M in **1b**. Repetitive wavelength scans in the range of 240–600 nm showed that the reaction followed a first-order pattern. Absorbance versus time data were taken at 325 nm. The data were fit to a standard first-order rate equation to provide  $k_{\text{obs}}$ .

(45) (a) Thompson, L. H.; Wu, R. W.; Felton, J. S. *Proc. Natl. Acad. Sci. U.S.A.* **1991**, *88*, 3827–3831. (b) Pfau, W.; Martin, F. L.; Cole, K. J.; Venitt, S.; Phillips, D. H.; Grover, P. L.; Marquardt, H. *Carcinogenesis* **1999**, *20*, 545–551.

(46) Novak, M.; Pelecanou, M.; Roy, A. K.; Andronico, F. M.; Plourde, F. M.; Olefirowicz, T. M.; Curtin, T. J. *J. Am. Chem. Soc.* **1984**, *106*, 5623–5631.

(47) Novak, M.; Brodeur, B. A. *J. Org. Chem.* **1984**, *49*, 1142–1144.

All kinetics of the decomposition of **1b** in the presence of the added  $\text{N}_3^-$  were performed in 0.02 M 1/2 NaH<sub>2</sub>PO<sub>4</sub>/Na<sub>2</sub>HPO<sub>4</sub> buffers at pH 6.8 under ionic strength and temperature conditions identical to those of the kinetic studies done in the absence of  $\text{N}_3^-$ . NaN<sub>3</sub> solutions were prepared at high concentration (0.45 M) in a 0.02 M phosphate buffer at the appropriate pH and were diluted into the working range with a 0.02 M phosphate buffer of the same pH and ionic strength. Repetitive wavelength scans showed consecutive first-order behavior. Absorbance versus time data were collected at 335 nm and fit to a consecutive first-order rate equation by nonlinear least-squares procedures.

**Product Analysis.** Reaction products obtained in the absence of  $\text{N}_3^-$  were monitored by HPLC with UV detection at 308 nm. HPLC conditions were C<sub>18</sub> reverse-phase analytical column, 65:35 MeOH/H<sub>2</sub>O eluent, at a flow rate of 1.0 mL/min. For preparative scale isolation, a ca.  $9.3 \times 10^{-3}$  M was prepared in 8 mL of DMF. This solution was added to 50 mL of pH 7.0, 0.02 M phosphate buffer at 20 °C in 270  $\mu\text{L}$  aliquots at 40 s intervals. The reaction was continued for 10 half-lives (400 s) after the last addition of **1b**. HPLC indicated that **1b** had decomposed. The solution was extracted with CH<sub>2</sub>Cl<sub>2</sub> ( $3 \times 25$  mL). The organic extracts were dried over anhydrous Na<sub>2</sub>SO<sub>4</sub>, and the solvent was evaporated. The residue was dissolved in MeOH, filtered to remove insoluble materials, and purified by preparative HPLC. The purified products were identified as **5** and **12** by comparison with authentic samples (see Supporting Information).

The product studies of the decomposition of **1b** in the presence of  $\text{N}_3^-$  was performed in 0.02 M 1/2 NaH<sub>2</sub>PO<sub>4</sub>/Na<sub>2</sub>HPO<sub>4</sub> buffers at pH 6.8 under ionic strength and temperature conditions identical to the kinetic studies. Products were monitored by HPLC with UV detection at 335 nm. HPLC conditions were identical to those described above. The initial concentration of **1b** was adjusted so that  $\text{N}_3^-$  was kept in at least a 10-fold excess in all experiments. Product yields were determined by the average of two HPLC injections taken after 8 half-lives of the slower of the two reactions detected by kinetics. Isolation and characterization of the  $\text{N}_3^-$  adduct, **16**, are described in the Supporting Information.

**Acknowledgment.** The 500 MHz NMR spectrometer and the LC/MS were provided by grants to MU by the Hayes Investment Fund of the Ohio Board of Regents.

**Supporting Information Available:** Synthesis and characterization of **6**, **7**, **1b**, and **12**, isolation and characterization of **16**, spectrophotometric titration of **1b**, kinetic data for **1b**, <sup>1</sup>H and <sup>13</sup>C NMR spectra for **1b**, **12**, and **16**, and plots of  $-\log \text{TD50}$  for mice and rats, including PhIP, versus log  $S$ . This material is available free of charge via the Internet at <http://pubs.acs.org>.

JO070306P